Journal of Taibah University of Science

https://www.tandfonline.com/journals/tusc20

Impact Factor = 3.3

Publisher = Taylor and Francis

Accepted September 22nd 2023.

Natural convection of nanofluid in a porous medium within a right-angle trapezoidal enclosure: A Tiwari-Das nanofluid model

Kothuru. Venkatadri[*1], Syed Fazuruddin[2], O. Anwar Bég[3] and Obbu Ramesh[4]

[1]*Department of Mathematics, Indian Institute of Information Technology Sri City, Chittoor-517464,* ***A.P., India.***
[2]*Department of Mathematics, Sreenivasa Institute of Technology and Management Studies, Chittoor- 517001* A.P., **India.**
[3]*Department of Aeronautical & Mechanical Engineering MPESG, Corrosion Lab, 3-08, SEE Building, School of Computing, Science and Engineering, University of Salford, Manchester, M54WT,* ***UK.***
[4]*Department of Mathematics, Siddartha Institute of Science and Technology, Puttur-517581,* ***A.P., India***
[*]*Corresponding author. Email: venkatadri.venki@gmail.com*

ABSTRACT

The study uses the Tiwari-Das nanofluid model to compute free convective flows in a right-angled trapezoidal cavity containing a porous material which is saturated with Cu-water nanofluid material. This investigation aims to enhance the characteristics of hybrid fuel cells and energy depository devices by analysing the cavity thermal physics and fluid flow characteristics. In the fuel cell trapezoidal enclosure geometry, the inclined and right wall portions are maintained at different isothermal temperatures, at all times. Finite difference-based stream function-vorticity numerical simulations are employed to carry out this analysis. The outcomes have been presented for isotherms, streamlines, and Nusselt numbers concerning nanoparticle volume fraction, Darcy number, and various Rayleigh numbers. It is found that the inverse relationship between the thermal Rayleigh number and the nanofluid volume has a significant impact on the average Nusselt number.

KEYWORDS: *Trapezoidal enclosure, Natural convection, Cu-water nanofluid, permeable medium, Numerical; Fuel cells.*

NOMENCLATURE

Roman Symbols

C_p *Specific heat at fixed pressure*

g *Gravitation acceleration vector*

K *Porous medium permeability*

k *Thermal conductivity*

P *Pressure*

Ra *Rayleigh number*

T_c *Temperature of Cold right wall*

T_h *Hot left wall temperature*

T *Temperature*

(u, v) *Cartesian velocity components*

(U, V) *Dimensionless velocity components*

V *Darcian velocity vector*

(x, y) *Cartesian co-ordinates*

(X, Y) *Dimensionless co-ordinates*

Greek

β *Coefficient of Thermal expansion.*

ϕ *Uniform concentration of the nanoparticles*

ψ *Stream function*

μ *Dynamic viscosity*

ρ *Density*

ε *Permeability of the porous medium*

θ *Non-dimensional temperature*

Subscripts

c *Cold*

f *Fluid*

h *Hot*

mnf *Nanofluid saturated porous medium*

m *Clear fluid saturated porous medium*

nf *Nano fluid*

s *Particle*

1. INTRODUCTION

Natural convection plays a significant role in several technologies and engineering analysis. It has several technical uses, including applications of solar systems, structures of civil engineering, the electronic sector, boilers used in industrial sectors and porous ovens. Convection heat transfer with permeable substances is now being studied in a variety of settings. The reason for this is that heat transmission in permeable substances has variety of applications ranging from biological transport phenomena to oil recovery sector in the petroleum industries. A variation in temperature between the solid matrix along with the percolate fluid has been examined and identified in the applications of permeable media such as the ecological effect of dumped nuclear waste, thermal power systems, chemical reactors, and so on. Further the impacts of thermal radiation in closed enclosures were studied in several research publications along with thermosolutal convection. Heat transfer through nanofluids has long been investigated both experimentally and conceptually. The origin of these concepts provides a precise and short explanation of the principles of enhancing heat transport. More over Nanofluids are a new type of fluids that form when stable nanoparticles interact with basic fluids. Nanofluids have several uses in building, research, manufacturing, and a variety of other industries.

In [1] studied the thermohydraulic characteristics of nanofluids moving across porous media distinct elements of three distinct convective heat transport techniques, specifically natural, forced convection and mixed convection, were studied, including second law analysis, MHD flow, thermophoresis, nanoparticle shape effect, non-Newtonian nanofluids, Brownian motion

and hybrid nanofluids. The primary findings of this study are provided in three sections: outcomes, difficulties, and future directions. Using a non-equilibrium thermal model, Sheremet et al. [2] conducted a computational analysis of free convective temperature distribution in an aluminium foam enclosure that has been differentially heated and is equipped with a Cu/water nanofluid. The study focused on the relationship between fluid flow and heat conduction and the Rayleigh number Ra, nano particles solid volume fraction, permeability of the porous field, and heat conduction at the nanofluid/solid matrix interface. Barman et al. [3] examined the result of enclosure aspect ratio on buoyancy driven fluid movement in a vertically situated curvy permeable enclosure with its wavy right wall kept at a constant less heat and heat source implanted at the vertical left end wall, leaving both the horizontal walls adiabatic. In this study for a constant aspect ratio, wall waviness, and heat source the flow-through Darcian permeable medium is influenced by convection as the Rayleigh-Darcy number augments. Because waviness resists the flow of fluid, midway vertical velocity decreases when the wave amplitude increases and the amount of variations per unit length, with the influence of a being more noticeable than the amount of variations per unit length. Thermal radiation and inclined magnetic fields have been studied by Abdelraheem et al. [4] for their effects on phase transition substance and thermosolutal convection inside a wavy horizontal enclosure equipped with NEPCMs-water mixes. At the primary time step, the time-fractional derivative has an effect on the zone of a phase change substance and minor changes has been found at the steady state. Increasing the nanoparticle concentration to 5% reduces the speed of nanofluid by 27.590%. Raising the Hartmann number also reduces the nano-fluid motions inside a wavy horizontal enclosure. Barnoon et al. [5] investigated movement of nanofluid and temperature distribution in a permeable cavity with a pair of cylinders incorporated in the enclosure existing and without existing the effect of thermal radiation. The findings indicate that changing the cavity angle might result in an increase or decrease in temperature distribution. Furthermore, taking thermal radiation into consideration, heat transmission is likely to be lesser than that which does not exist. Furthermore, the appropriate rate of temperature distribution is determined based on the conditions of temperature. Heat transmission can be enhanced or lowered by adjusting the cavity angle of the cylinders. Al-Kouzetal.[6] provided an experimental parametric investigation on free convective and entropy production inside an enclosure equipped with a nanofluid subjected to a field of magnetism in the existence of a permeable media. The most important points raised by this work are the temperature distribution in the cavity with the influence of flow regime (Ra), medium porosity Da, strength of magnetic field Ha, and heating length, which is defined by geometric parameters. It was also

noted that the effects intensity of each parameter given varies. Sheremet et al. [7] numerically deliberated free convective flow in a porous square cavity with opposing temperature atside walls along with adiabatic top and bottom walls equipped with a water-based nanofluid. In this article a Special consideration has been given to the impacts of the permeability of the porous field, nanoparticles solid volume fraction, Rayleigh number, and solid matrix of the permeable medium in the field of fluid flow, heat circulation and Nusselt number. The effects of diverse porosity on the transient temperature distribution of convective Cu-H2O fluid flow via a permeable field (crystal bead, sandstone and aluminium foam) within a trapezoidal shaped cavity with no thermal equilibrium state were investigated by Al-Weheibi et al. [8]. In contrast, the local thermal equilibrium condition of nanoparticles and ordinary fluid is taken into account. The effects of distinct permeability and porosity factors on the Nusselt numbers are discussed in depth. free convection of Cu-H_2O nanofluids surrounded by a permeable annulus generated in between the square cavity and an elliptical cylinder was investigated by Dogonchi et al. [9]. The outcomes of this article show that increasing the Ra and Da values significantly develop temperature distribution and the average Nusselt number at a given aspect ratio. Furthermore, increasing the Ra values enhances the momentum of nanofluid, but increasing the cylinder's aspect ratio which is in elliptical shape has an adverse effect. Mehryan et al. [10] studied the free convection of Ag-MgO hybrid or water nanofluid flow via a permeable cavity has been explored using the LTNE model. The Darcy model is used to investigate the flow dynamics of a permeable field. Distributing Ag-MgO hybrid nanoparticles reduces fluid flow potency and temperature distribution rate via both the phases (solid & fluid) of porous medium. Furthermore, the utilisation of hybrid nanoparticles reduces the LTNE state. A thorough numerical analysis of fluid momentum and temperature distribution in an enclosure with revolving obstacles of circular type consisting of permeable field and exposed to a magnetic force was conducted by Barnoon et al. [11]. The findings in this article shows that the thermal conditions of the round obstacles, as well as their orientation, have a considerable impact on the movement fluid and temperature distribution. The largest heat transmission rates are seen in cold circular obstacles, whereas the lowest are found in heated circular obstacles. Furthermore, the type of the permeable field and the magnetic field has an effect on the pace of temperature dispersion. Numerous pieces of literature [[12], [13], [14], [15]] exist that discuss the porous enclosure and its related work. A study conducted by Ellahi [16] investigated the MHD flow of nanofluid within a pipe at a higher temperature than the non-Newtonian fluid with variable viscosity. The study revealed that the MHD parameter reduces the fluid flow, and the velocity profile dominates the temperature profile even in varying viscosities. Ellahi [17]

also found that the velocity profile in pressurized alumina water near a wavy channel equipped with porous material was reduced. These findings offer valuable insights into fluid flow behaviour under different conditions. In a study by Bhatti et al. [18], the behaviour of tantalum and cobalt nano-particles in a hybrid fluid structure was investigated. The study found that the presence of Lorentz force led to a reduction in velocity. In their study; Tripathi et al. [19] presented a model for analysing the flow of electro-osmotic nanofluid in a micro channel with unique wave formations on the walls. The results of this study are crucial for comprehending the fluid dynamics of proposed innovative drug delivery devices. Akbar et al. [20] conducted a mathematical analysis of peristaltic momentum and heat transport in a heat-dependent variable-viscosity nanofluid flowing through a channel with heat generation and thermal buoyancy effect in the shape of cylinders, platelets and bricks. Tripathi et al. [21] developed analytical results for the flow characteristics of nanofluid in a heterogeneous channel. The findings of this study suggest that thermophoresis accelerates transverse flow and reduces pressure variations.

This particular work has the potential to significantly advance our knowledge and comprehension of heat transfer and nanomaterials, which can be of great use for academic research purposes. Furthermore, the outcomes of this study can be applied in the advancement of heat transformers, particularly those that are commonly utilized in electronic components. The outcomes of this project can enhance and broaden the understanding of heat transfer and materials, which can be utilized for academic purposes. Additionally, these findings can be utilized in the advancement of heat transformers, particularly those utilized in electronic gadgets and fuel cells.

2. MATHEMATICAL FORMULATION

The nanoparticle diluted Newtonian 2-dimensional laminar flow, enclosed in a porous medium right angled trapezoidal enclosure is considered in the present work. Figure. 1aexhibits the geometrical representation for the computational configuration. Assume the enclosure embedded with porous medium with constant thermo-physical properties. The horizontal walls of the enclosure are thermally insulated, the left inclined wall is isothermally cold while the opposite walls is isothermally constant high temperature is maintained. By assuming a Boussinesq approximation, very small densities, and so the incompressibility constraints are

not violated, as well as the buoyancy force. Thermal radiation, external magnetic field, internal heat generation, and viscous dissipation are ignored in the analysis.

The set of governing equations laminar incompressible nanofluid taking into account in the conservation equation of mass, momentum, thermal transport and Poisson can be expressed as follows [22, 25]:

$$\frac{\partial \bar{u}}{\partial \bar{x}} + \frac{\partial \bar{v}}{\partial \bar{y}} = 0 \tag{1}$$

$$\rho_{nf}\left(\frac{\partial \bar{u}}{\partial t} + \bar{u}\frac{\partial \bar{u}}{\partial \bar{x}} + \bar{v}\frac{\partial \bar{u}}{\partial \bar{y}}\right) = -\frac{\partial p}{\partial \bar{x}} + \mu_{\mathrm{nf}}\left(\frac{\partial^2 \bar{u}}{\partial \bar{x}^2} + \frac{\partial^2 \bar{u}}{\partial \bar{y}^2}\right) - \frac{\mu_{\mathrm{nf}}}{k}\bar{u} \tag{2}$$

$$\rho_{nf}\left(\frac{\partial \bar{v}}{\partial t} + \bar{u}\frac{\partial \bar{v}}{\partial \bar{x}} + \bar{v}\frac{\partial \bar{v}}{\partial \bar{y}}\right) = -\frac{\partial p}{\partial \bar{y}} + \mu_{\mathrm{nf}}\left(\frac{\partial^2 \bar{v}}{\partial \bar{x}^2} + \frac{\partial^2 \bar{v}}{\partial \bar{y}^2}\right) - \frac{\mu_{\mathrm{nf}}}{k}\bar{v} + \mathrm{g}\,(\rho\beta)_{\mathrm{nf}}(\mathrm{T} - \mathrm{T_c}) \tag{3}$$

$$\frac{\partial T}{\partial t} + \bar{u}\frac{\partial T}{\partial \bar{x}} + \bar{v}\frac{\partial T}{\partial \bar{y}} = \alpha_{nf}\left(\frac{\partial^2 T}{\partial \bar{x}^2} + \frac{\partial^2 T}{\partial \bar{y}^2}\right) \tag{4}$$

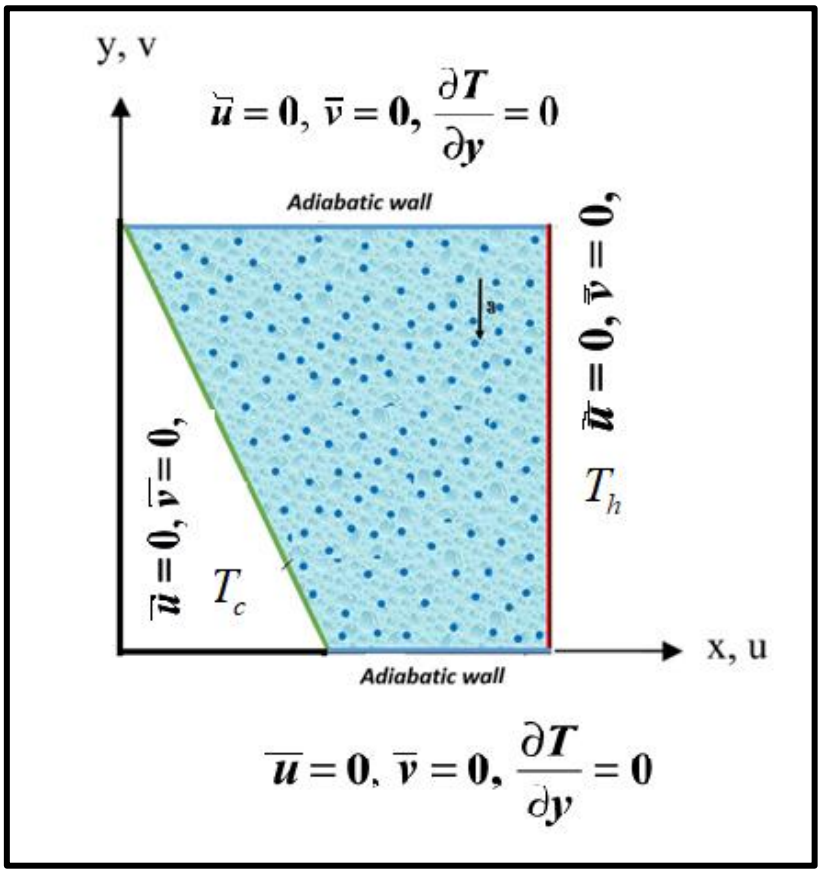

Figure. 1a. Schematic diagram of computational configuration

The wall boundary constraints of the trapezoidal cavity as follows:

On left inclined wall: $\bar{u} = \bar{v} = 0, \mathrm{T} = \mathrm{T_c}$

On right wall: $\bar{u} = \bar{v} = 0, \mathrm{T} = \mathrm{T_h}$

On horizontal adiabatic walls: $\bar{u} = \bar{v} = \frac{\partial T}{\partial \bar{y}} = 0$

With the pleasure eliminating vorticity-stream function approach and considered the below dimensionless quantities:

$$x = \frac{\bar{x}}{L}, y = \frac{\bar{y}}{L}, \quad u = \frac{\bar{u}L}{\alpha}, v = \frac{\bar{v}L}{\alpha}, \quad \psi = \frac{\bar{\psi}}{\alpha}, \quad \omega = \frac{L^2\bar{\omega}}{\alpha}, \tau = \frac{t\alpha}{L^2}, \theta = \frac{T-T_c}{T_h-T_c} \tag{5}$$

Where the nanofluid parameters are

$$\mu_{nf} = \mu_f(1 + 4.93\emptyset + 222.4\emptyset^2)$$

$$\rho_{nf} = (1-\emptyset)\rho_f + \emptyset\rho_p,$$

$$(\rho_c)_{nf} = (1-\emptyset)(\rho_c)_f + \emptyset(\rho_c)_p \tag{6}$$

$$(\rho\beta)_{nf} = (1-\emptyset)(\rho\beta)_f + \emptyset(\rho\beta)_p$$

$$k_{nf} = k_f(1 + 2.944\emptyset + 19.67\emptyset^2)$$

Stream function ψ and vorticity ω in non-dimensional form

$$u = \frac{\partial \psi}{\partial y}, v = -\frac{\partial \psi}{\partial x}, w = \frac{\partial v}{\partial x} - \frac{\partial u}{\partial y} \tag{7}$$

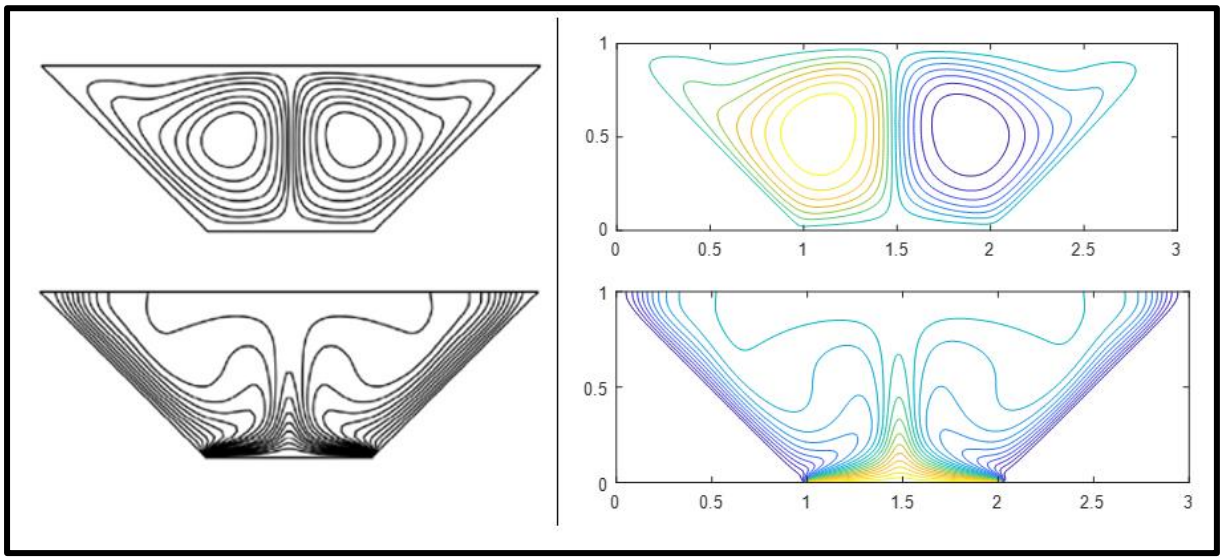

.

Figure. 1b. Comparison results of streamlines and temperature contours of (left- previous study) [23] and (right- present result)

Therefore, the equations that govern (4)-(7) can be expressed in a dimensionless format.

$$\frac{\partial^2\psi}{\partial x^2}+\frac{\partial^2\psi}{\partial y^2}=-\omega \tag{8}$$

$$\frac{\partial\omega}{\partial\tau}+\frac{\partial\psi}{\partial y}\frac{\partial\omega}{\partial x}-\frac{\partial\psi}{\partial x}\frac{\partial\omega}{\partial y}=H_1(\emptyset)\,Pr\left(\frac{\partial^2\omega}{\partial x^2}+\frac{\partial^2\omega}{\partial y^2}\right)-H_1(\emptyset)\frac{Pr}{Da}\,\omega+H_2(\emptyset)\,Ra\,Pr\left(\frac{\partial\theta}{\partial x}\right) \tag{9}$$

$$\frac{\partial\theta}{\partial\tau}+\frac{\partial\psi}{\partial y}\frac{\partial\theta}{\partial x}-\frac{\partial\psi}{\partial x}\frac{\partial\theta}{\partial y}=H_3(\emptyset)\left(\frac{\partial^2\theta}{\partial x^2}+\frac{\partial^2\theta}{\partial y^2}\right) \tag{10}$$

Here Prandtl number $\mathrm{Pr}=\frac{\mu_f}{\rho_f\alpha_f}$, Thermal Rayleigh number $\mathrm{Ra}=\frac{g\mu_f\beta_f(T_h-T_c)L^3}{\rho_f\alpha_f}$Darcy parameter $\mathrm{Da}=\frac{k}{L^2}$,$H_1(\phi)=\frac{1+4.93\phi+222.4\phi^2}{1-\phi+\phi\rho_p/\rho_f}$, $H_2(\phi)=\frac{1-\phi+\phi(\rho\beta)_p/(\rho\beta)_f}{1-\phi+\phi\rho_p/\rho_f}$ and $H_3(\phi)=\frac{1+2.944\phi+19.67\phi^2}{1-\phi+\phi(\rho_c)_p/(\rho_c)_f}$. All the symbols and parameter are addressed in nomenclature. **Table 1** presents a comprehensive analysis of the thermophysical characteristics of nanofluids. The coupled partial differential equations have been employed with the following boundary conditions:

At right hot wall: $\psi=0,\quad\theta=1$

At cold inclined cold wall: $\psi=0,\quad\theta=0$

Top and bottom wall (thermally insulated walls): $\psi=0,\quad\frac{\partial\theta}{\partial y}=0$

Table. 1. Composed water and Cooper (Cu) nanoparticle's thermal-physical characteristics

(see [24])

Physical characteristics	Base fluid (water)	Cu
$C_p(J.kg^{-1}.K^{-1})$	4179	385
$\rho(kg.m^{-3})$	997.1	2700
$k(W.m^{-1}.K^{-1})$	0.613	205
$\alpha\times10^{-7}(m^2.s^{-1})$	1.47	846.4
$\beta\times10^{-5}(K^{-1})$	21	2.22

Table. 2. Comparison of average Nusselt number (Nu) with *Pr*=0.71(air)

Ra	Nu	Ref. [26]	Ref. [27]	Ref. [28] FEM	Present study (FDM)
10^3	Average	1.12	1.074	1.117	1.1185
10^4	Average	2.243	2.084	2.254	2.2526
10^5	Average	4.52	4.3	4.598	4.5907
10^6	Average	8.8	8.743	8.976	8.9905

3. COMPUTATIONAL METHOD OF SOLUTION AND CODE VALIDATION

In order to address the complex problem of non-linear transportation equations (8) - (10) and meet the required wall conditions, we employed a second-order approximation method based on finite difference techniques. Specifically, we utilized a central difference scheme to accurately approximate the diffusion and convective terms involved in the equations. This approach allowed us to arrive at a viable solution through a systematic and iterative process. To obtain numerical approximated integral for the nonlinear momentum and energy equations, a linear relaxation method was used to solve the discretized equations obtained through finite difference scheme. To obtain quick and accurate results for the stream function, the Gauss-Seidel scheme is adopted to solve the discretization equation of the Poisson equation. Further details can be found in references [19, 20, 21, 22]. In all simulation processes, we make use of an under-relaxation parameter value of 10^{-1}, ensuring that the calculations are carried out in a smooth and effective manner. Additionally, we set the convergence criteria at a value of 10^{-4}, guaranteeing a high level of accuracy and precision in the resulting output.

It is important to mention that there is currently no experimental research data available that can fully simulate the problem. In the study conducted by Gibanov et al. [23], **Figure 1b** displays the findings of free convective fluid momentum in a trapezoidal cavity using a working fluid of Pr = 0.71 and Ra = 10^5. The study compared the results obtained from the commercial FLUENT software with the ones derived from their own developed computational code. Our research, on the other hand, evaluated the current numerical finite difference method (FDM) and compared it to the findings of Gibanov et al. [23]. Based on the results presented in **Figure 1b,** it is evident that our findings align well with the existing literature. The finite difference approach was developed in an in-house MATLAB-based platform and verified with

previous numerical research [33-35]. Table.2. displays the average Nusselt number near the hot wall over a wide range of Ra ($Ra=10^3 - 10^6$). An excellent correlation of present numerical method with the [26-28]. As a result, we can confidently use our numerical method to further investigate the problem discussed in this paper.

4. RESULTS AND DISCUSSION

In this study, we investigate the mechanism of coupled fluid flow and heat transmission via free convection within a trapezoidal cavity containing a permeable field saturated with Cu-Water nanofluid. The buoyancy forces created by density gradients drive the mixture, resulting in the formation of streamlines and isotherms throughout the cavity. We investigate the effect of various controlling factors within a certain range $10^3 \leq Ra \leq 10^6$, $10^{-4} \leq Da \leq 10^{-1}$, $0.01 \leq \phi \leq 0.05$ and fixed Pr = 6.2, tested, including buoyancy parameter, and Darcy number.

In **Figure 2**, we can observe the streamlined contours for various Rayleigh numbers (Ra). One can easily notice stream function value increases from the Rayleigh number intensifications. It should be noted that even a little raise in the Rayleigh number can have a big influence on the stream function. In fact, as the Ra value rises, so does the buoyancy force, which improves the stream function. The larger flow of the cavity is observed at the centre and the flow sucking towards the inclined cold wall from the straight hot wall of the cavity that causes the flow function to increase. By raising the Ra from 10^3 to 10^6, a strong vortex forms at the cavity's centre. By enhancing the Ra, the vortex grows and is drawn to its full potential, exposing much of the cavity to the maximum flow towards the slant wall where the streamlines are highly clustered near the cold wall.

Figure 3 depicts the impact of Ra on the isotherms. Buoyancy forces are frequently more intense at large Ra due to the greater kinetic energy of the flow. Ra increases temperature and concentration distributions through trapezoidal cavities due to enhanced buoyancy forces. As a result, there is a strong heat dispersion between the hot and cold walls, and the corresponding asymmetric thermal contours are clearly visible. As Ra grows, heat transmission becomes increasingly advection-dominated, and the isotherm field deforms as buoyancy increases. Circulation is lowest towards the wall and highest near the centre. As a result of the initiation of advection, the isotherms deviate substantially and are pushed towards the inclined wall with higher Ra. Temperature variations along the hot and cold walls appear to be critical for the formation of the thermal boundary layer at $Ra = 10^6$. Small temperature gradients can be seen

at the centre regime due to more circulation there, whereas a big temperature stratification zone can be found at the vertical symmetry line due to flow stagnation.

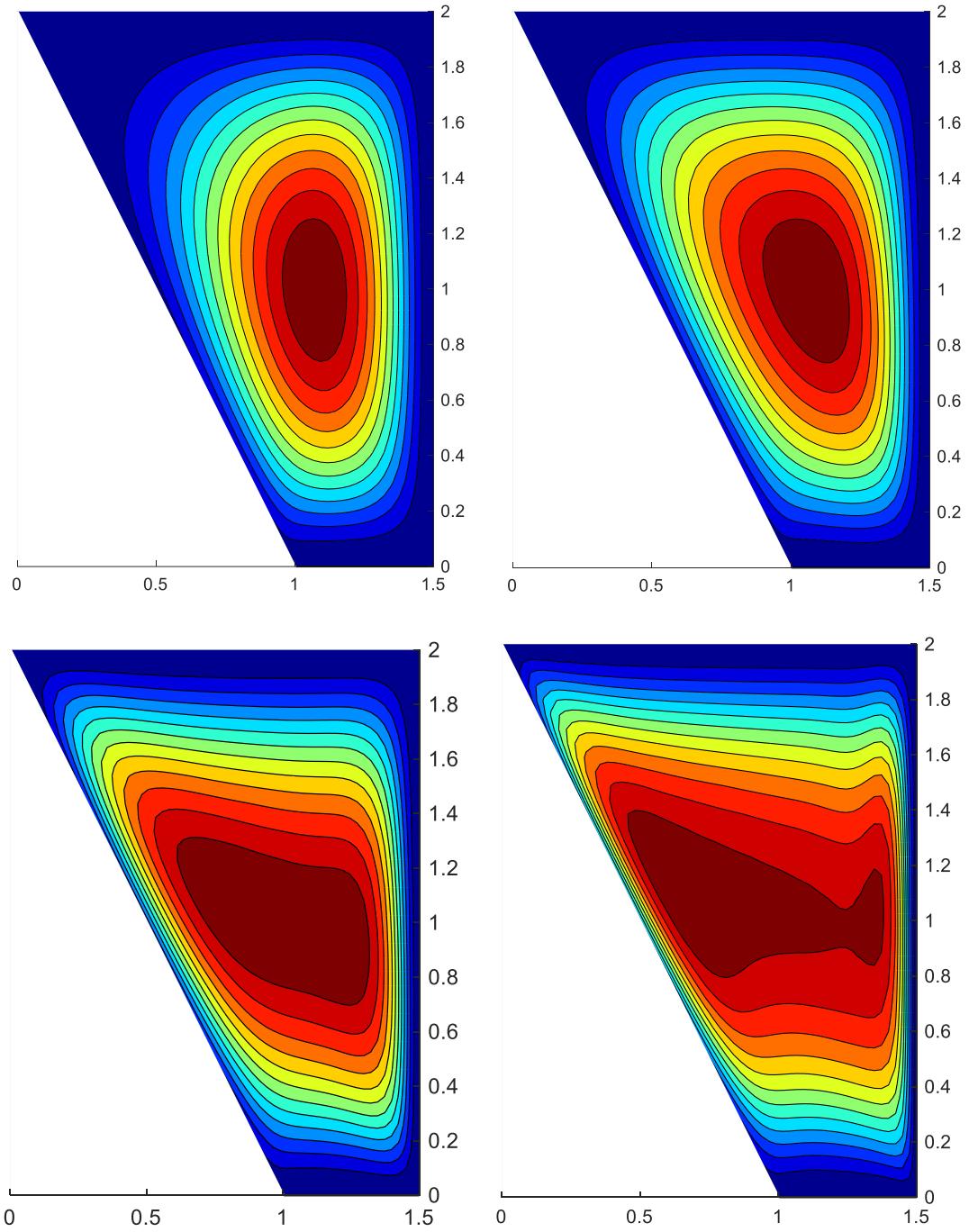

Figure. 2. Streamlines for distinct values of Rayleigh number Ra (Ra = 10^3-10^6) with Darcy number Da = 0.01, nano particle volume fraction parameter Φ = 0.04.

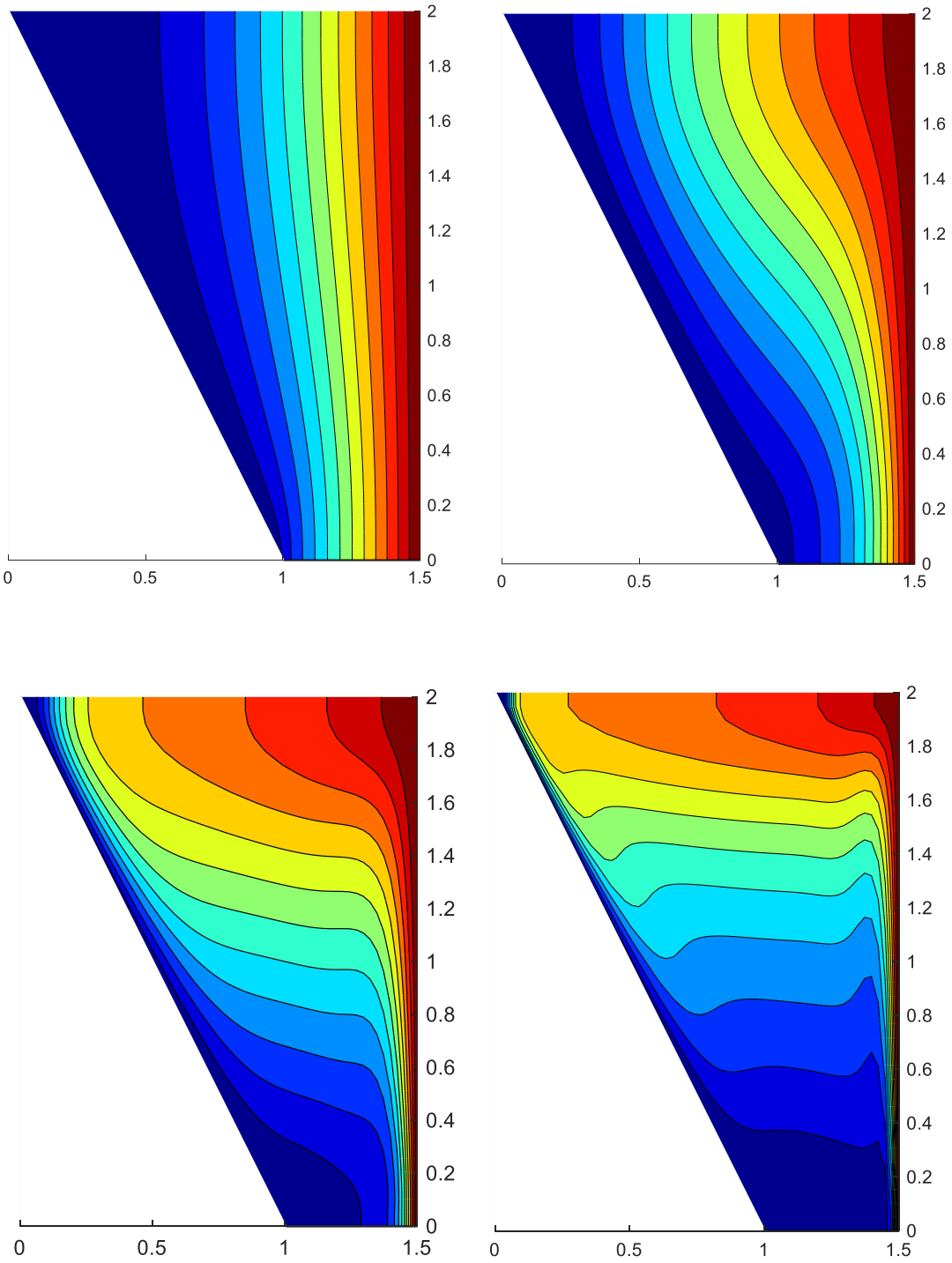

Figure. 3.Isotherms for distinct values of Rayleigh number Ra (Ra = 10^3-10^6) with Darcy number Da = 0.01, nano particle volume fraction parameter Φ = 0.04

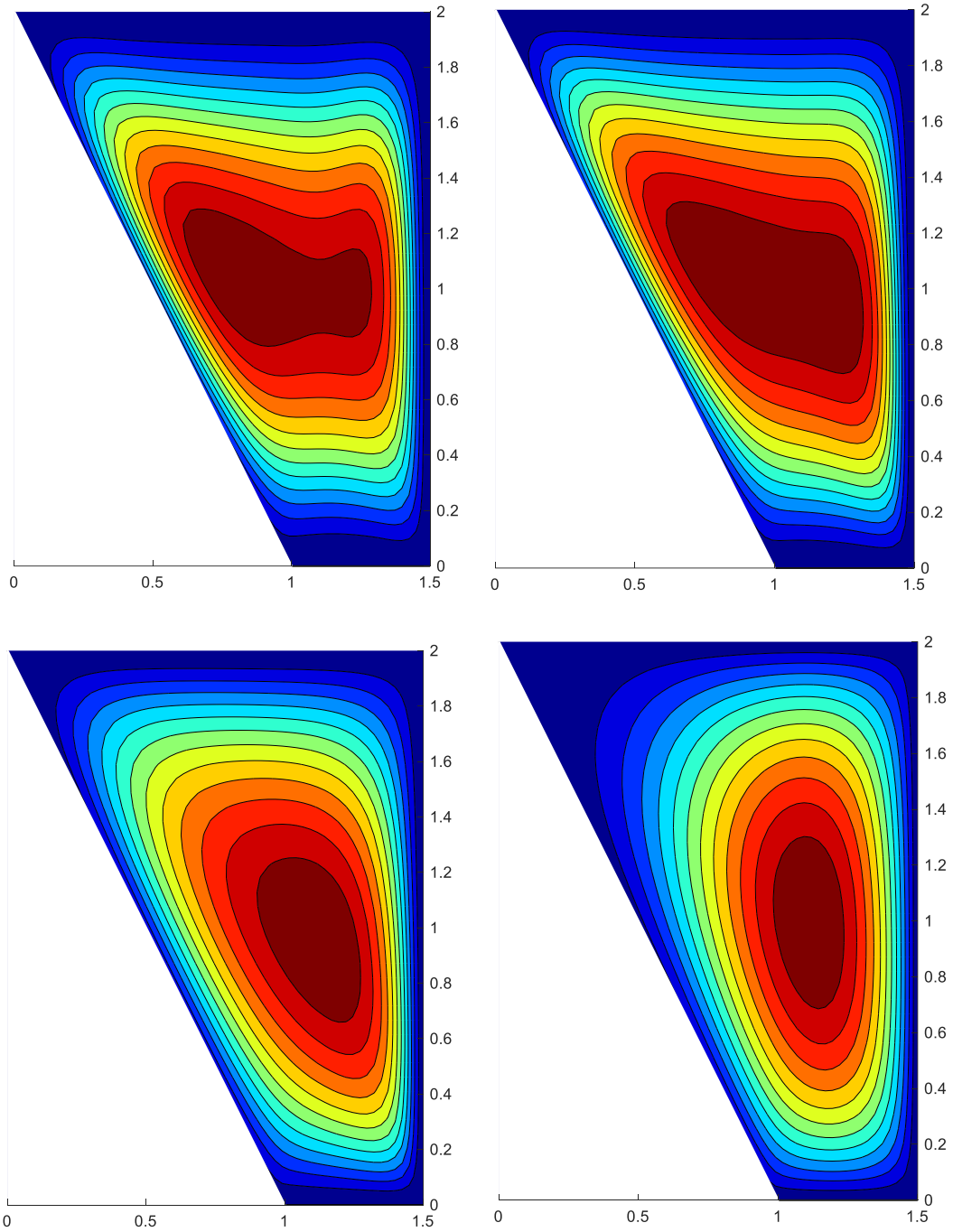

Figure. 4. Streamlines for various values of Darcy number Da (Da= 0.1-0.0001) with Rayleigh number Ra =10^5 and nano particle volume fraction parameter Φ = 0.04

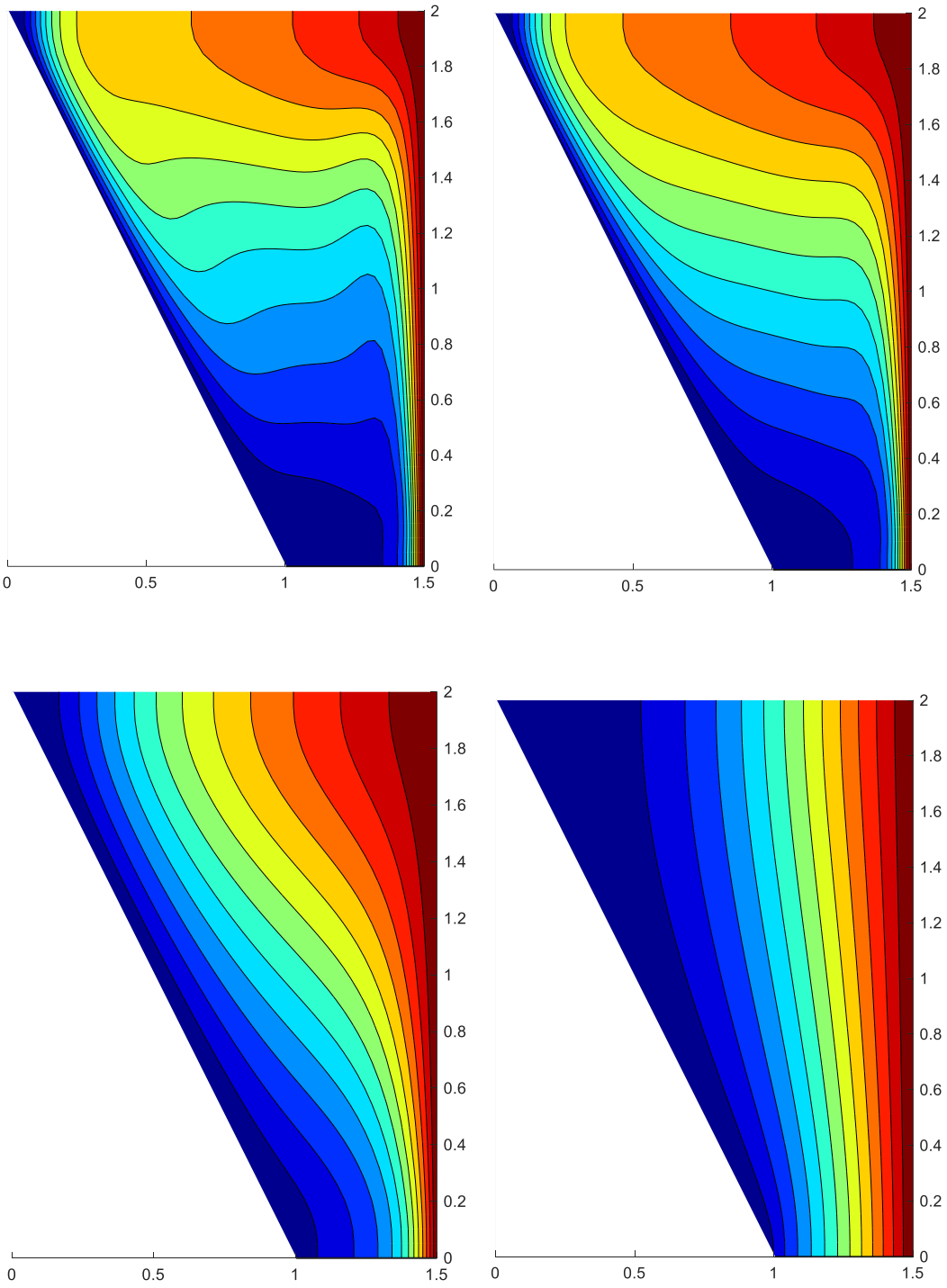

Figure. 5. Isotherms for distinct values of Darcy number Da (Da= 0.1-0.0001) with Rayleigh number Ra =105 and nano particle volume fraction parameter Φ = 0.04

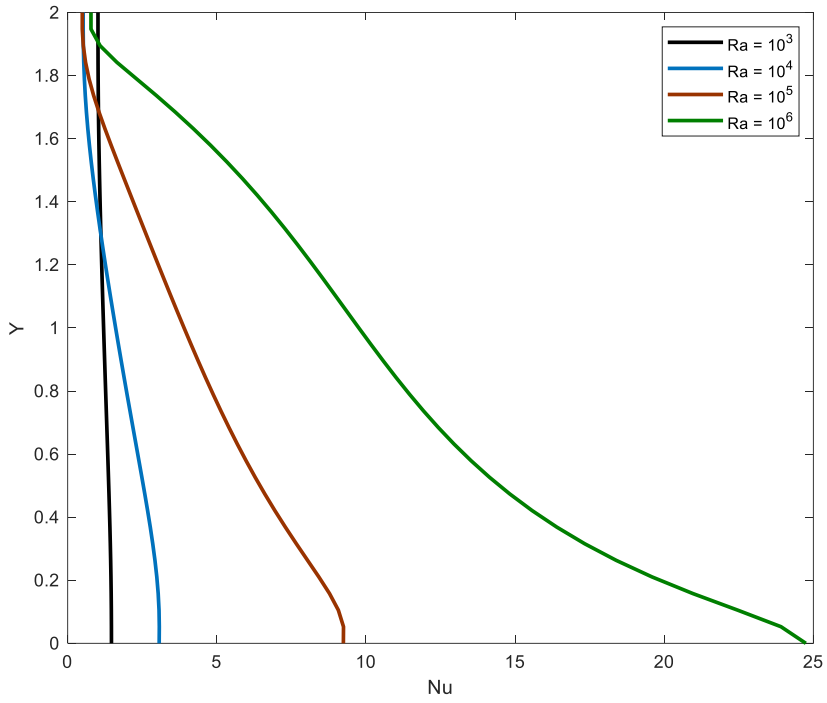

Figure. 6. Local Nusselt number of hot wall (right) for Darcy number Da = 0.01, nano particle volume fraction parameter Φ = 0.04

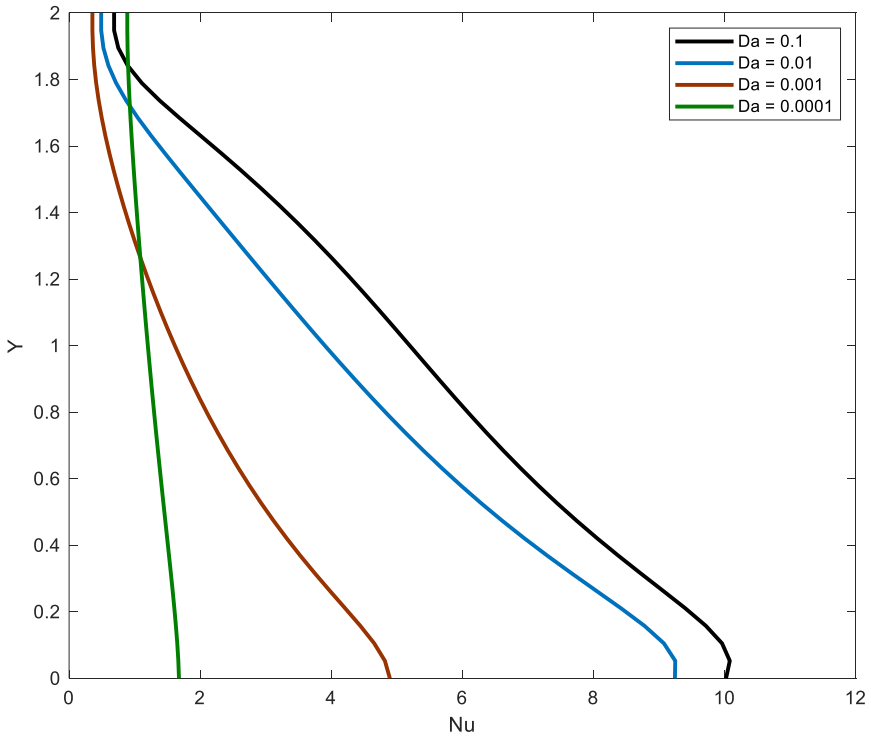

Figure. 7 Local Nusselt number of hot wall (right) for Rayleigh number Ra =10^5 and nano particle volume fraction parameter Φ = 0.04.

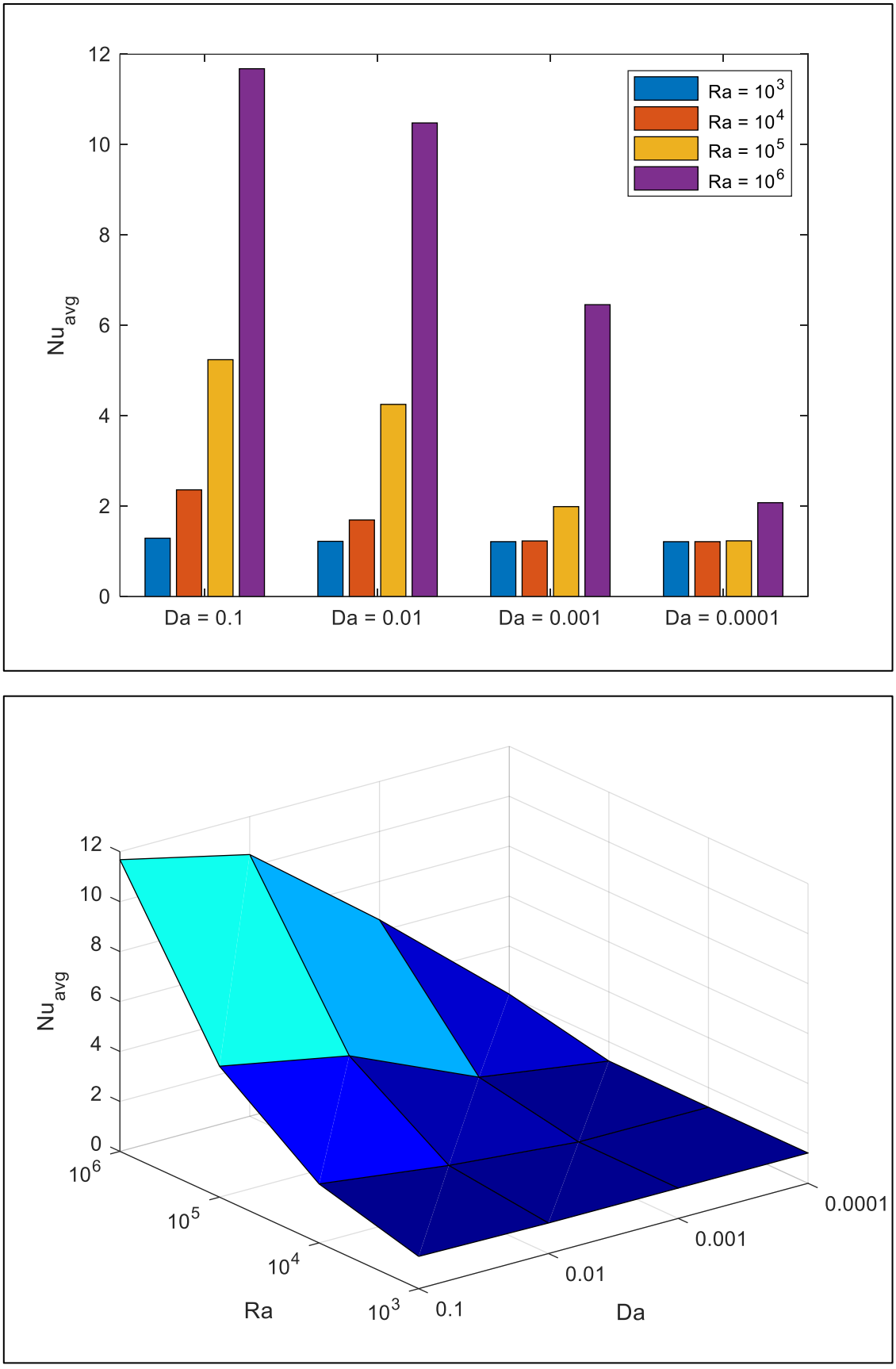

Figure. 8. Average Nusselt number along the hot wall with nano particle volume fraction parameter Φ = 0.04.

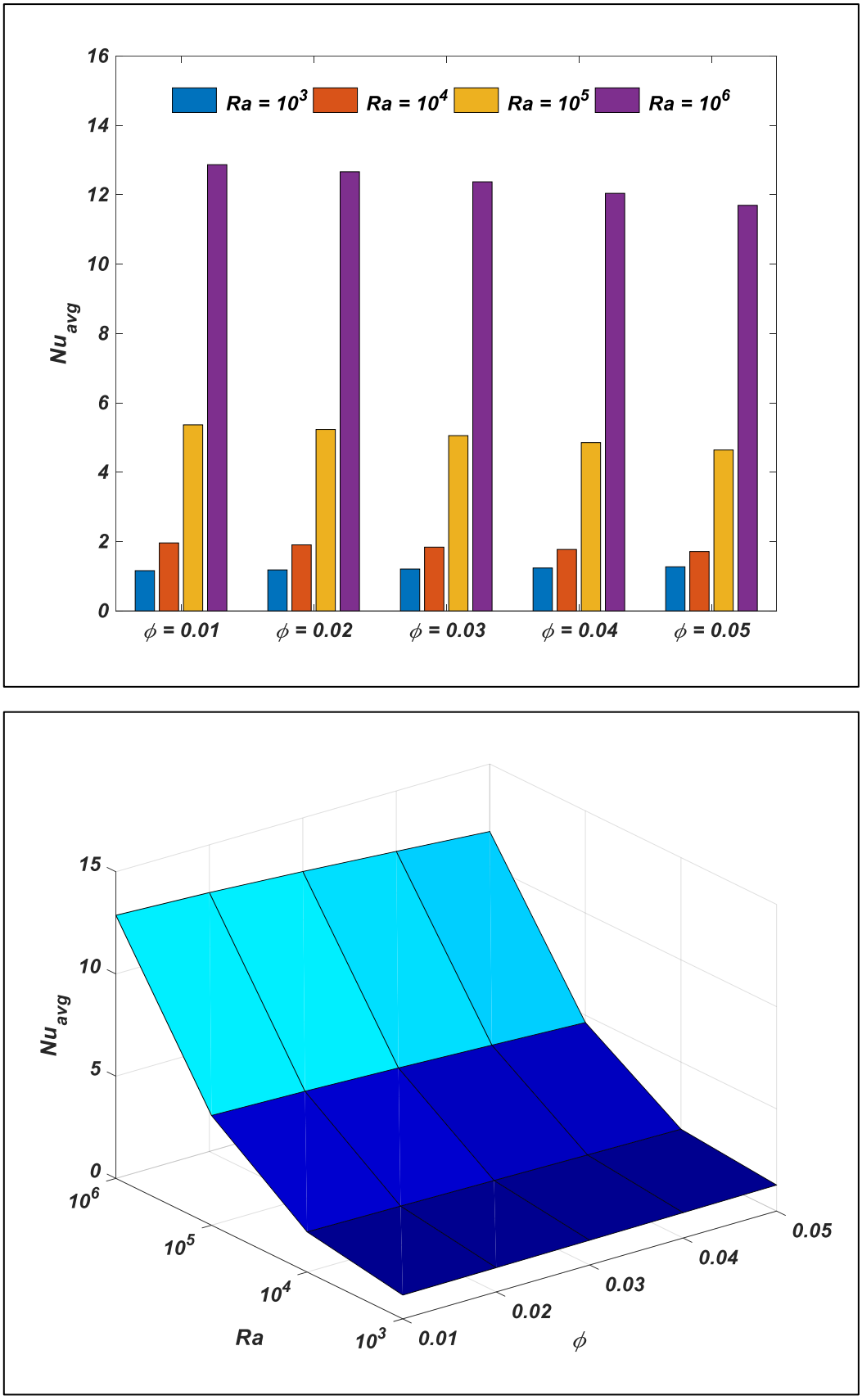

Figure. 9. Average Nusselt number along hot wall with permeability parameter Da = 0.01.

Figure 4 displays the contours of streamlines for different Darcy numbers (Da). The streamlines show a single clockwise flow across the porous zone when Da value is lower. However, as the Da value increases, the flow rate spreads throughout the porous area, which is influenced by the harmonic motion of the fluid. As can be observed, a decline in Da number causes high porous resistance, which in turn causes the flow function in the cavity to decline. Low porosity results in a greater solid surface of porous matrix within the cavity, which reduces fluid movement. As a result, in such circumstances, the ability of fluid circulation is diminished, and fluid flow is impeded. The vortex's intensity within the cavity is also controlled by permeability, which can grow or decrease as a result of the buoyancy parameter Ra. In this case, the reverse trend of rising Ra values may be observed for the decrementing value of Da. Furthermore, the decrease in permeability leads the streamlines to be more regular, resulting in improved fluid circulation inside the trapezoidal cavity.

Figure 5 depicts the isotherms for various Da levels. As the Da value decreases, the thermal boundary layers become thinner. Furthermore, when permeability decreases, more cold thermal plumes escape to the left of the heated wall, aiding in the cooling process. Temperature distributions inside a trapezoidal cavity are reduced when the Da number is reduced. As permeability diminishes, the isotherm-lines become more regular, improving fluid circulation in the cavity. When Da=0.1(high permeability) the isotherms are very much closer to both the vertical walls when compared to Da=0.0001 (low permeability), which shows high Da has higher temperature gradient. We investigated the association between the thermal Rayleigh number, porosity, and the local Nusselt number in this work (**Fig 6**). Our findings indicate that the heat transport along the hot wall increases with the growth in the Rayleigh number. This means that an intensification in the thermal Rayleigh number leads to enhanced temperature distribution from the heated wall. Moreover, we observed that the transient mean Nu raises with the Darcy-Rayleigh number. This suggests that the greater the Darcy-Rayleigh number, the better the temperature distribution from the hot wall. Additionally, we found that the local Nusselt number raised with thermal buoyancy parameter Ra at the heated wall. However, for low Rayleigh numbers such as 10^3 and 10^4, the local Nusselt number does not show a significant change. These observations provide valuable insights into the mechanisms of temperature expansion in porous field and can be utilized to optimize thermal management systems in various applications of engineering. This is due to conduction's dominance. At large Rayleigh numbers, however, the average Nusselt number rapidly increases. This tendency is particularly observed for Rayleigh numbers of 10^5 and 10^6.

As depicted in **Figure 7**, the variation in Local Nusselt number experiences a gradual delay in steep increase as the Da value decreases. At a low Da value the heat transfer reaches the physical limit of an almost impenetrable porous medium. Decreasing Da value from 0.1 to 0.0001 decreases the local Nusselt number which means reduction of porosity suppresses the flow and heat expansion rate. On the basis of information provided in **Figure 8**, it may be noticed that correlation exists in between the Nusselt number and Rayleigh and Darcy parameters. Specifically, as the Ra value rises and the Da value drops, the temperature distribution rate is also seen to increase. This suggests that there exists an inverse association between the average Nusselt number and both Ra and Da values. **Figure 9** depicts a thorough illustration of the relationship between the thermal Rayleigh number, the average Nusselt number, and the nanofluid volume fraction. The plot elucidates that an increment in the nanofluid volume fraction leads to a diminution in the rate of heat transfer. Conversely, an increase in the thermal Rayleigh number results in an increase in the rate of heat transmission. These observations signify the significant impact of both nanofluid volume fraction and thermal Rayleigh number in heat expansion.

5. FINAL REMARKS

This research paper provides an in-depth investigation of free convection flows inside a right-angle trapezoidal cavity. The Tiwari and Das nanofluid model was utilized to simulate the flow, while the cavity itself was equipped with a porous bed and a Cu-water nanofluid. The investigation was carried out through numerical simulations, allowing for a comprehensive and detailed understanding of the fluid dynamics within the system. The outcomes of this analysis provide valuable information on the behaviour of natural convection flows in complex geometries and highlight the potential of nanofluids for augmenting heat transfer in practical applications. We analysed the impact of various governing parameters within the range $10^3 \leq Ra \leq 10^6$, $10^{-4} \leq Da \leq 10^{-1}$, $0.01 \leq \phi \leq 0.05$ and fixed $Pr = 6.2$, tested, including buoyancy parameter, and Darcy number.This study has identified the following noteworthy results:

- The value of the stream function increases as the Rayleigh number increases, indicating that the Rayleigh number has a major impact on the stream function.
- With an increase in Ra, advection will probably have a more significant impact on heat transportation.

- As permeability decreases, streamlines become more regular, resulting in greater fluid circulation in the cavity.
- Decreasing the Da number declines the temperature distributions inside a trapezoidal cavity; nevertheless, the average Nusselt number rapidly increases with high Rayleigh numbers.
- The thermal Rayleigh number and the volume fraction of nanofluid have an inverse effect on the average Nusselt number.

DISCLOSURE STATEMENT

No potential conflict of interest was reported by the author(s).

REFERENCES

[1] *M. Hemmat Esfe, M. Bahiraei, H. Hajbarati, M. Valadkhani, A comprehensive review on convective heat transfer of nanofluids in porous media: Energy-related and thermohydraulic characteristics. Applied Thermal Engineering. 2020: 178: 115487.doi.org/10.1016/j.applthermaleng.2020.115487*

[2] *M.A. Sheremet, I. Pop, R. Nazar, Natural convection in a square cavity filled with a porous medium saturated with a nanofluid using the thermal nonequilibrium model with a Tiwari and Das nanofluid model. International Journal of Mechanical Sciences. 2015; 100:312-321. doi.org/10.1016/j.ijmecsci.2015.07.007*

[3] *Barman, P., & Rao, P. S., Effect of aspect ratio on natural convection in a wavy porous cavity submitted to a partial heat source. International Communications in Heat and Mass Transfer. 2021; 126:105453. doi.org/10.1016/j.icheatmasstransfer.2021.105453*

[4] *Abdelraheem M. Aly, Zehba Raizah, Shreen El-Sapa, Hakan F. Oztop, Nidal Abu-Hamdeh, Thermal diffusion upon magnetic field convection of nano-enhanced phase change materials in a permeable wavy cavity with crescent-shaped partitions. Case Studies in Thermal Engineering . 2022; 31:101855, doi.org/10.1016/j.csite.2022.101855*

[5] *Barnoon, P., Toghraie, D., Dehkordi, R. B., & Afrand, M.,Two phase natural convection and thermal radiation of non-Newtonian nanofluid in a porous cavity considering inclined cavity and size of inside cylinders. International Communications in Heat and Mass Transfer. 2019; 108:104285. doi.org/10.1016/j.icheatmasstransfer.2019.104285*

[6] *Al-Kouz, W., Aissa, A., Koulali, A. et al., MHD darcy-forchheimer nanofluid flow and entropy optimization in an odd-shaped enclosure filled with a (MWCNT-Fe_3O_4/water) using galerkin finite element analysis. Sci Rep. 2021; 11:22635.doi.org/10.1038/s41598-021-02047-y*

[7] *M. A. Sheremet T, Grosan I. Pop, Free Convection in a Square Cavity Filled with a Porous Medium Saturated by Nanofluid Using Tiwari and Das' Nanofluid Model. Transp Porous Med. 2015; 106:595–610. doi.org/10.1007/s11242-014-0415-3*

[8] *Al-Weheibi, S.M., Rahman, M.M. & Saghir, M.Z., Impacts of Variable Porosity and Variable Permeability on the Thermal Augmentation of Cu–H_2O Nanofluid-Drenched Porous Trapezoidal Enclosure Considering Thermal Nonequilibrium Model. Arab J Sci Eng. 2020; 45:1237–1251.doi.org/10.1007/s13369-019-04234-6*

[9] *Dogonchi, A.S., Nayak, M.K., Karimi, N. et al., Numerical simulation of hydrothermal features of Cu–H_2O nanofluid natural convection within a porous annulus considering diverse configurations of heater. J Therm Anal Calorim. 2020; 141:2109–2125.doi.org/10.1007/s10973-020-09419-y*

[10] *S.A.M. Mehryan, M. Ghalambaz, A.J. Chamkha, et al., Numerical study on natural convection of Ag–MgO hybrid/water nanofluid inside a porous enclosure: A local thermal non-equilibrium model. Powder Technology. 2019; 367(1):443-455. doi.org/10.1016/j.powtec.2020.04.005*

[11] *Barnoon, P., Toghraie, D. &Karimipour, A. Application of rotating circular obstacles in improving ferrofluid heat transfer in an enclosure saturated with porous medium subjected to a magnetic field. J Therm Anal Calorim. 2021; 145:3301–3323. doi.org/10.1007/s10973-020-09896-1*

[12] *Al-Farhany, Khaled, et al., Numerical investigation of natural convection on Al2O3–water porous enclosure partially heated with two fins attached to its hot wall: under the MHD effects. Applied Nanoscience. 2023; 13(1):555-572.doi.org/10.1007/s13204-021-01855-y*

[13] *Abderrahmane, Aissa, et al., Investigation of the free convection of nanofluid flow in a wavy porous enclosure subjected to a magnetic field using the Galerkin finite element method. Journal of Magnetism and Magnetic Materials. 2023; 569: 170446.doi.org/10.1016/j.jmmm.2023.170446*

[14] *Chordiya, J., & Sharma, R. V., Numerical analysis of the longitudinal size of the partition on natural convection heat transfer and fluid flow within a differentially heated porous enclosure. Heat Transfer. 2023; 52(1):890-910.doi.org/10.1002/htj.22721*

[15] *Hosseinzadeh, K., Moghaddam, M. E., Nateghi, S., Shafii, M. B., & Ganji, D. D., Radiation and convection heat transfer optimization with MHD analysis of a hybrid nanofluid within a wavy porous enclosure. Journal of Magnetism and Magnetic Materials. 2023; 566: 170328.doi.org/10.1016/j.jmmm.2022.170328*

[16] *Ellahi, R. The effects of MHD and temperature dependent viscosity on the flow of non-Newtonian nanofluid in a pipe: Analytical solutions. Applied Mathematical Modelling. 2013; 37(3): 1451–1467. doi:10.1016/j.apm.2012.04.004*

[17] *Ellahi, R., Sait, S. M., Shehzad, N., & Ayaz, Z. A hybrid investigation on numerical and analytical solutions of electro-magnetohydrodynamics flow of nanofluid through porous media with entropy generation. International Journal of Numerical Methods for Heat & Fluid Flow. 2019; 30(2): 834–854. doi:10.1108/hff-06-2019-0506*

[18] *M.M. Bhatti, Sara, Abdelsalam. Scientific Breakdown of a Ferromagnetic Nanofluid In Hemodynamics: Enhanced Therapeutic Approach. Mathematical Modelling of Natural Phenomena. Math. Model. Nat. Phenom.2022: 17: 44. doi.org/10.1051/mmnp/2022045*

[19] *Tripathi, D., Sharma, A., & Anwar Bég, O. Joule heating and buoyancy effects in electro-osmotic peristaltic transport of aqueous nanofluids through a microchannel with complex wave propagation. Advanced Powder Technology. 2018; 29(3): 639–653. doi: 10.1016/j.apt.2017.12.009*

[20] *Akbar, N. S., Huda, A. B., Habib, M. B., & Tripathi, D. Nanoparticles shape effects on peristaltic transport of nanofluids in presence of magnetohydrodynamics. Microsystem Technologies. 2018. doi:10.1007/s00542-018-3963-6*

[21] *Tripathi, D., Bhushan, S., Bég, O. A., & Akbar, N. S. Transient peristaltic diffusion of nanofluids: A model of micropumps in medical engineering. Journal of Hydrodynamics. 2018; 30(6):1001–1011. doi: 10.1007/s42241-018-0140-4.*

[22] *K Venkatadri., Visualization of thermo-magnetic natural convective heat flow in a square enclosure partially filled with a porous medium using bejan heatlines and Hooman energy flux vectors: Hybrid fuel cell simulation. Geoenergy Science and Engineering.2023; 224:211591. doi.org/10.1016/j.geoen.2023.211591*

[23] *Gibanov, N. S., Sheremet, M. A., & Pop, I., Free convection in a trapezoidal cavity filled with a micropolar fluid. International Journal of Heat and Mass Transfer. 2016; 99:831-838. doi.org/10.1016/j.ijheatmasstransfer.2016.04.056*

[24] *Vedavathi, N., Venkatadri, K., Fazuruddin, Sd., and Raju, G.S.S., Natural Convection Flow in Semi-Trapezoidal Porous Enclosure Filled with Alumina-Water Nanofluid Using Tiwari*

and Das' Nanofluid Model. Engineering Transactions. 2022; 70(4):303-318.doi.org/10.24423/EngTrans.1285.20221004

[25] *Venkatadri, K. Radiative magneto-thermogravitational flow in a porous square cavity with viscous heating and Hall current effects: A numerical study of ψ–v scheme. Heat Transfer.2022; 51 (7):6705-6723. doi.org/10.1002/htj.22619*

[26] *D. de Vahl Davis, Natural convection of air in a square cavity: a benchmark solution, Int. J. Numer. Meth. Fluids. 1983; 3: 249-264.*

[27] *M. T. Manzari, An explicit finite element algorithm for convective heat transfer problems, Int. J. Numer. Meth. Heat Fluid Flow.1999; 9: 860-877.*

[28] *D. C. Wan, B. S. V. Patnaik and G. W. Wei, A new benchmark quality solution for the buoyancy-driven cavity by discrete singular convolution, Numerical Heat Transfer, Part B. 2001; 40: 199-228.*